

Interpretation of moiré phenomenon in the image domain

Lingsheng Kong,^{1,2} Sheng Cai,¹ Zongxuan Li,^{1,2} Guang Jin,^{1,*} Shangbing Huang,^{1,2}
Kai Xu,¹ and Tiancong Wang^{1,2}

¹Changchun Institute of Optics, Fine Mechanics and Physics, Chinese Academy of Sciences, Changchun 130033, China;

²Graduate School of the Chinese Academy of Science, Beijing 100039, China;
*jing@ciomp.ac.cn

Abstract: We propose an interpretation of moiré phenomenon in the image domain. The interpretation is basically based on the analysis of the waveform of the line families. The period, angle, and intensity profile of moiré fringes can be obtained directly in the image domain according to this interpretation. Moreover, pseudo-moiré can be interpreted visually with the consideration of the illusional contrast of the human visual system. The interpretation, which is consistent with the Fourier theory when the two superposed gratings are periodic, involves only the image domain and shows remarkable simplicity, just like the indicial equation method.

©2011 Optical Society of America

OCIS codes: (070.0070) Fourier optics; (050.2770) Gratings; (120.4120) Moiré techniques.

References and links

1. M. Abolhassani and M. Mirzaei, "Unification of formulation of moiré fringe spacing in parametric equation and Fourier analysis methods," *Appl. Opt.* **46**(32), 7924–7926 (2007).
2. L. Rayleigh, "On the manufacture and theory of diffraction gratings," *Philos. Mag.* **4**, 81–93 (1874).
3. G. Oster, M. Wasserman, and C. Zwerling, "Theoretical Interpretation of Moiré patterns," *J. Opt. Soc. Am. A* **54**(2), 169–175 (1964).
4. A. J. Durelli and V. J. Parks, *Moiré Analysis of Strain* (Prentice-Hall, Englewood Cliffs, New Jersey, 1970).
5. K. Patorski, *Handbook of the Moiré Fringe Technique* (Elsevier, Amsterdam, 1993).
6. O. Bryngdahl, "Moiré: formation and interpretation," *J. Opt. Soc. Am. A* **64**(10), 1287–1294 (1974).
7. O. Bryngdahl, "Moiré and higher grating harmonics," *J. Opt. Soc. Am. A* **65**(6), 685–694 (1975).
8. I. Amidror and R. D. Hersch, "The role of Fourier theory and of modulation in the prediction of visible moiré effects," *J. Mod. Opt.* **56**(9), 1103–1118 (2009).
9. I. Amidror, *The Theory of the Moiré Phenomenon* (Springer-Verlag, London, 2009), Chap.2.
10. G. Lebanon and A. M. Bruckstein, *Designing Moiré Patterns* (Springer-Verlag, Berlin, 2001).
11. K. Patorski, S. Yokozeki, and T. Suzuki, "Moiré profile prediction by using Fourier series formalism," *Jpn. J. Appl. Phys.* **15**(3), 443–456 (1976).
12. I. Amidror and R. D. Hersch, "Mathematical moiré models and their limitations," *J. Mod. Opt.* **57**(1), 23–36 (2010).

1. Introduction

The moiré phenomenon has been known for a long time. The term moiré comes from French, where it refers to watered silk. The moiré silk consists of two layers of fabric pressed together. As the silk bends and folds, the two layers shift with respect to each other, causing the appearance of interfering patterns. Generally, superposition of two or more periodic (or quasi-periodic) structures leads to a coarser structure, named moiré pattern or moiré fringe [1].

Modern scientific research into the moiré phenomenon and its application started only in the second half of the 19th century with pioneering works, such as Lord Rayleigh pointed out that two overlapped 1D-gratings can produce a set of low-frequency fringes which is relevant to quality of the gratings in 1874 [2].

Various methods are reported in the literature for modeling and analyzing the moiré phenomenon. Among these methods, the indicial equation method and the Fourier theory are used most widely. The simplest and probably also the oldest method for analyzing the

geometric shape of moiré fringes in the superposition of two given curvilinear gratings is the indicial (or the parametric) equation method [3–5]. This method, which involves only the image domain, is based on the curve equations of the original curvilinear gratings: If each of the original layers is regarded as an indexed family of lines (or curves), the moiré fringe that results from their interaction forms a new indexed family of lines (or curves), whose equations can be deduced from the equations of the original layers.

The first significant step in the introduction of the Fourier theory to moiré phenomenon can be traced back to the 1960s. The Fourier theory which can systematically interpret the properties of moiré fringes in overlapped repetitive structures was eventually shown to be more effective due to the complexity of the previous classical algebraic and geometric analysis [6,7]. The Fourier theory approach enables us to analyze properties not only in the original layers and their superposition but also in their spectral representations, and thus offers a more profound insight into the problem. Therefore, the Fourier theory provides indispensable tools for exploring moiré phenomenon.

The high-frequency moiré fringe, which cannot be seen by human eyes (namely, outside the visibility circle), can be obtained through theoretical calculation of the Fourier theory, which indicates the superiority of utilizing mathematical model in explaining physical or experimental phenomenon. However, the pseudo-moiré, whose frequency cannot be captured by the Fourier theory [8], can be seen by human eyes. Therefore, the limitation of the Fourier theory is obvious for the pseudo-moiré.

Pseudo-moiré may occur in various circumstances, even in multiplicative superposition. Some plausible classical answers are given in [8] (Issac Amidror's work) as follows:

- The effect of non-linearity;
- Microstructure versus macrostructure;
- The human visual system;
- Modulation.

In this work, we propose an interpretation for moiré phenomenon, which differs from the indicial equation method and Fourier theory, in the image domain. Based on the variation characteristic of the superposition of two unidimensional waves with different phases, we can find out the family of parallel straight lines, whose average intensity in the direction normal to the family of parallel straight lines varies periodically. This family of lines corresponds to the real moiré in the Fourier theory. At the same time, there exists the family of lines, which possess the illusional average intensity variation in the direction normal to the family of parallel straight lines. This causes illusional contrast in human visual system and produces the pseudo-moiré. The pseudo-moiré, which is firstly studied in 2009 [8], can be explained visually in the image domain through the proposed interpretation. Coincident with the traditional Fourier theory [9], the interpretation of moiré phenomenon applies visible and quantitative analysis to pseudo-moiré from two aspects: one is the crest distribution and envelope profile of average intensity, while the other is the human visual system.

2. Theoretical framework of the interpretation in the image domain

2.1 Multiplication of two unidimensional cosinusoidal waves

Generally, superposition of two and more periodic (or quasi-periodic) structures leads to moiré fringes. It is well known that the superposition of two cosinusoidal gratings is the simplest way to produce moiré fringes. For simplicity, our proposed interpretation will be explained mostly based on the superposition of two cosinusoidal gratings. The interpretation is fundamentally based on the analysis of fluctuations of average intensity of the line families, so the waveform of the arbitrary line in the superposition of two cosinusoidal gratings can be expressed as the superposition of two unidimensional cosinusoidal waves. Thus, we firstly analyze the waveform of the superposition of two unidimensional waves.

The profile and average intensity of the multiplication of two unidimensional cosinusoidal waves relate to their frequencies and the relative phase shift φ . The two unidimensional cosinusoidal waves and their multiplication are given by

$$T_1 = \frac{1}{2}(\cos 2\pi x + 1), \quad T_2 = \frac{1}{2}[\cos[\frac{2\pi}{t}(x + \varphi)] + 1], \quad (1)$$

$$T = T_1 \times T_2 = \frac{1}{2}(\cos 2\pi x + 1) \times \frac{1}{2}[\cos[\frac{2\pi}{t}(x + \varphi)] + 1] \\ = \frac{1}{8}\cos[2\pi(\frac{t+1}{t}x + \frac{\varphi}{t})] + \frac{1}{8}\cos[2\pi(\frac{t-1}{t}x - \frac{\varphi}{t})] + \frac{1}{4}\cos(2\pi x) + \frac{1}{4}\cos[\frac{2\pi}{t}(x + \varphi)] + \frac{1}{4}. \quad (2)$$

Because of the reciprocity between T_1 and T_2 , we only focus on the circumstance, where t is a rational number that greater than or equal to 1. According to Eq. (2), we can conclude that T is a periodic function. Here, M is designated as the period of T , and the value of M is discussed for two circumstances.

When $t = 1$,

$$T = \frac{1}{8}\cos[2\pi(2x + \varphi)] + \frac{1}{8}\cos(2\pi\varphi) + \frac{1}{4}\cos(2\pi x) + \frac{1}{4}\cos[2\pi(x + \varphi)] + \frac{1}{4} \quad (3)$$

So $M = 1$. The average intensity I_{avr} of T is given by

$$I_{avr} = \frac{1}{M} \int_0^M T dx = \int_0^1 \frac{1}{8}[\cos(2\pi\varphi) + 2] dx = \frac{1}{8}(\cos 2\pi\varphi + 2). \quad (4)$$

M equals the least common multiple of $\frac{t}{t+1}$, $\frac{t}{t-1}$, and t in the case of $t > 1$. Thus, the average intensity I_{avr} of T is given by

$$I_{avr} = \frac{1}{M} \int_0^M T dx = \frac{1}{4} \quad (5)$$

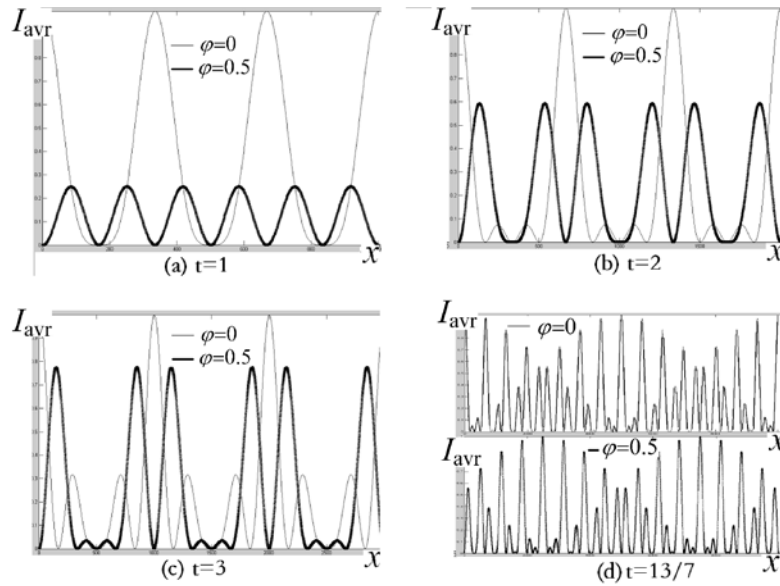


Fig. 1. The waveform of the function T with the variable t when $\varphi = 0$ and $\varphi = 0.5$.

It can be seen that: when $t = 1$, the average intensity I_{avr} relates to φ ; when $t > 1$, the average intensity is constant with different φ . The simulations of the waveforms that vary with t are shown in Fig. 1 (the regular threads correspond to $\varphi = 0$ and the bold threads correspond to $\varphi = 0.5$).

It is seen from Fig. 1 that when $t = 1$, the average intensity I_{avr} varies due to φ ; when t is a rational number greater than 1, the average intensities I_{avr} with different φ are the same, but the distribution and envelope of the wave crests are different. Here, we introduce a parameter defined by human-eye recognition: the illusional contrast. In the circumstance, where $t > 1$ and if human eyes can distinguish the wave crests and the envelope of the crests with different φ , we define that there exists an illusional contrast for the t .

2.2 The physical meaning of the interpretation

The simplest and oldest model for analyzing the geometric shape of moiré fringes in the superposition of two curvilinear gratings is the indicial (or parametric) equation method. This model is based on the curve equations of the original curvilinear gratings. If each of the original layers is regarded as an indexed family of curves, the moiré fringe of the superposition forms a new indexed family of curves, whose equations can be inferred from the equations of the original gratings [10].

Similar as the indicial equation method, we propose an interpretation, which involves only the image domain, to explain the formation of moiré fringe. As shown in Fig. 2, the pitches of the two gratings are P_1 and P_2 respectively, and the included angle of two gratings is α (α is a small angle). The arbitrary line A is drawn and the included angles between A and the two gratings are β and γ respectively ($\alpha + \beta + \gamma = \pi$). The equivalent periods of the two gratings along the orientation A are $P'_1 = P_1 / \sin \gamma$ and $P'_2 = P_2 / \sin \beta$ respectively. So the waveform T_A in the direction to the line A is the superposition of two unidimensional waves whose periods are P'_1 and P'_2 respectively. The line B parallels to A at a distance of h , as shown in Fig. 2. According to the Fig. 2, we can conclude that the waveform T_B in the direction to the line B has the relative phase shift $R + L$ comparing to the waveform T_A . Thus the waveform of every single line, which parallels to the orientation A, has different relative phase shift. When average intensity of the line family varies periodically in the direction normal to line A, the

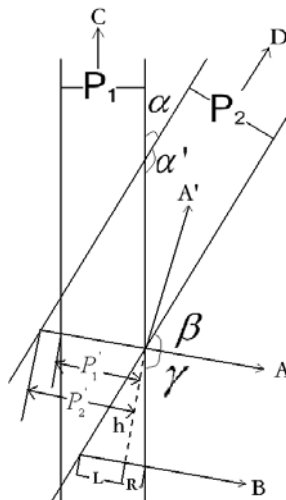


Fig. 2. Schematic of the interpretation of the moiré phenomenon in the image domain

fluctuation of average intensity as the macrostructure is captured by human eyes namely moiré phenomenon. Accordingly, the orientation of moiré corresponds to the direction along the line A and the period of moiré is the distance between two lines whose average intensity is equal at their maximum (or minimum). In addition, the intensity profile of moiré can be obtained from the fluctuation of average intensity of the line family. The waveform along the direction C or D is a superposition of a constant wave and periodic wave, so the waveforms, which vary periodically in the orientation perpendicular to C and D, correspond to the two original gratings.

Based on the results of the superposition of two unidimensional waves, and the interpretation of moiré phenomenon in the image domain and references [8] [9], three inferences are given as shown below:

- The moiré fringes seen by human eyes are divided into two types: real moiré and pseudo-moiré. Real moiré describes the circumstance where exists the periodic variation of average intensity of the line family. Pseudo-moiré describes the circumstance where exists the illusional average intensity variation namely the illusional periodic fringe.
- As a transformation from the whole image domain to the frequency domain, the Fourier transform only reflects the periodic information of the holistic average intensity namely the periodic fringe of real moiré. When $t = 1$, there exists the periodic variation of the average intensity, and the moiré effects correspond to the frequency of the Fourier theory. When $t \neq 1$, the illusional intensity distribution corresponds to the pseudo-moiré with illusional contrast.
- In the orientations which are perpendicular respectively to the original gratings C or D, there also exists the periodic variation of average intensity. Thus the two orientations belong to the real moiré. In this paper, we only focus on the newly generated real moiré fringes (namely the $\pm(\vec{f}_1 - \vec{f}_2)$ and $\pm(\vec{f}_1 + \vec{f}_2)$ in Fourier theory).

In the following, the real moiré and pseudo-moiré are calculated from the interpretation of moiré phenomenon in the image domain. Because of the reciprocity between P_1 and P_2 , we denote that $P_1 < P_2$.

(a) Real moiré

Here $P_1 = P_2 = P'$, namely,

$$\frac{P_1}{\sin \gamma_r} = \frac{P_2}{\sin \beta_r} \quad (6)$$

$$\frac{P_2}{P_1} = \frac{\sin \beta_r}{\sin \gamma_r} = \frac{\sin(\pi - \alpha - \gamma_r)}{\sin \gamma_r} = \frac{\sin(\alpha + \gamma_r)}{\sin \gamma_r} = \sin \alpha \cot \gamma_r + \cos \alpha \quad (7)$$

Thus

$$\tan \gamma_r = \frac{P_1 \sin \alpha}{P_2 - P_1 \cos \alpha}, \quad \tan \beta_r = \frac{P_2 \sin \alpha}{P_1 - P_2 \cos \alpha}. \quad (8)$$

In a like manner ($\alpha + \alpha' = \pi$),

$$\tan \gamma_r' = \frac{P_1 \sin \alpha'}{P_2 - P_1 \cos \alpha'} = \frac{P_1 \sin \alpha}{P_2 + P_1 \cos \alpha}, \quad \tan \beta_r' = \frac{P_2 \sin \alpha'}{P_1 - P_2 \cos \alpha'} = \frac{P_2 \sin \alpha}{P_1 + P_2 \cos \alpha}. \quad (9)$$

When $R + L = P'$, the perpendicular distance between line A and line B is P_r (namely the period of real moiré):

$$R + L = P_r \cot \gamma_r + P_r \cot \beta_r = \frac{P_1}{\sin \gamma_r} = \frac{P_2}{\sin \beta_r} \quad (10)$$

We obtain

$$P_r = \frac{P_1 P_2}{\sqrt{P_1^2 + P_2^2 - 2P_1 P_2 \cos \alpha}}, \quad P_r' = \frac{P_1 P_2}{\sqrt{P_1^2 + P_2^2 + 2P_1 P_2 \cos \alpha}}. \quad (11)$$

The above angular and periodic expressions correspond to $\pm(\vec{f}_1 - \vec{f}_2)$ and $\pm(\vec{f}_1 + \vec{f}_2)$ in Fourier theory.

(b) Pseudo-moiré

Here $mP_1' = P_2'$ (m is an integer and greater than 1), in a like manner,

$$\frac{mP_1}{\sin \gamma_p} = \frac{P_2}{\sin \beta_p} \quad (12)$$

$$\frac{P_2}{mP_1} = \frac{\sin \beta_p}{\sin \gamma_p} = \frac{\sin \alpha \cos \gamma_p + \cos \alpha \sin \gamma_p}{\sin \gamma_p} = \sin \alpha \cot \gamma_p + \cos \alpha \quad (13)$$

We obtain

$$\tan \gamma_p = \frac{mP_1 \sin \alpha}{P_2 - mP_1 \cos \alpha}, \quad \tan \beta_p = \frac{P_2 \sin \alpha}{mP_1 - P_2 \cos \alpha}. \quad (14)$$

When $R + L = P_1'$, the perpendicular distance between line A and line B is P_p' (namely the period of pseudo-moiré):

$$R + L = P_p \cot \gamma_p + P_p \cot \beta_p = P_1 / \sin \gamma_p \quad (15)$$

We obtain

$$P_p = \frac{P_1 P_2}{\sqrt{m^2 P_1^2 + P_2^2 - 2mP_1 P_2 \cos \alpha}}, \quad P_p' = \frac{P_1 P_2}{\sqrt{m^2 P_1^2 + P_2^2 + 2mP_1 P_2 \cos \alpha}}. \quad (16)$$

The general moiré formulas of two cosinusoidal gratings are given by

$$\tan \gamma = \frac{mP_1 \sin \alpha}{P_2 \mp mP_1 \cos \alpha}, \quad P_m = \frac{P_1 P_2}{\sqrt{m^2 P_1^2 + P_2^2 \mp 2mP_1 P_2 \cos \alpha}}. \quad (17)$$

Generally speaking, the real moiré, which corresponds to $\pm(\vec{f}_1 - \vec{f}_2)$ and $\pm(\vec{f}_1 + \vec{f}_2)$ in the Fourier theory, is obtained when $m = 1$. The pseudo-moiré is produced when m is a rational number, greater than 1.

3. Simulations and verification

3.1 Little inclined cosinusoidal gratings with frequency ratios 1:1 ($P_1 = P_2 = P$)

The transmittance functions of two gratings are given by

$$r_1(x, y) = \frac{1}{2} \cos(2\pi f_1 x) + \frac{1}{2}, \quad r_2(x, y) = \frac{1}{2} \cos(2\pi f_2 [x \cos \theta_2 + y \sin \theta_2]) + \frac{1}{2}, \quad (18)$$

where $f_1 = f_2 = 1/P$; the superposition of two gratings is given in Fig. 3.

Here the real moiré formula in Eq. (17) coincides with the Fourier theory. Besides the original frequencies \vec{f}_1 and \vec{f}_2 , there are four frequency items which are vector sums

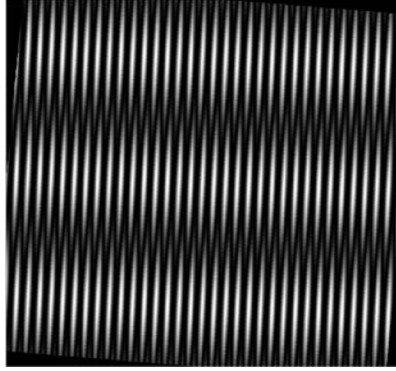


Fig. 3. The multiplicative superposition of two little inclined cosinusoidal gratings with frequency ratio 1:1

$\pm(\vec{f}_1 - \vec{f}_2)$ and vector differences $\pm(\vec{f}_1 + \vec{f}_2)$. The items $\pm(\vec{f}_1 - \vec{f}_2)$ correspond to the low-frequency moiré fringes in Fig. 3. The orientation of the fringes is at one-half the relative inclination of the two cosinusoidal gratings, and the period P_m of the fringes equals to $P/2|\sin(\alpha/2)|$. Based on the interpretation in section 2.2, we can also infer that equivalent pitches of the two gratings are equal in the orientation of one-half the relative inclination of the two gratings.

3.2 Little inclined cosinusoidal gratings with frequency ratios 1:2

Here $P_2 = 2P_1, f_1 = 1/P_1, f_2 = 1/P_2$.

Based on the analysis of the Fourier theory, there are four frequency items which are vector sums $\pm(\vec{f}_1 + \vec{f}_2)$ and vector differences $\pm(\vec{f}_1 - \vec{f}_2)$ besides the original frequencies \vec{f}_1 and \vec{f}_2 . But the low-frequency fringe is not captured in the Fourier theory as shown in Fig. 4(a). In the following, we analyze the phenomenon utilizing the interpretation in section 2.2.

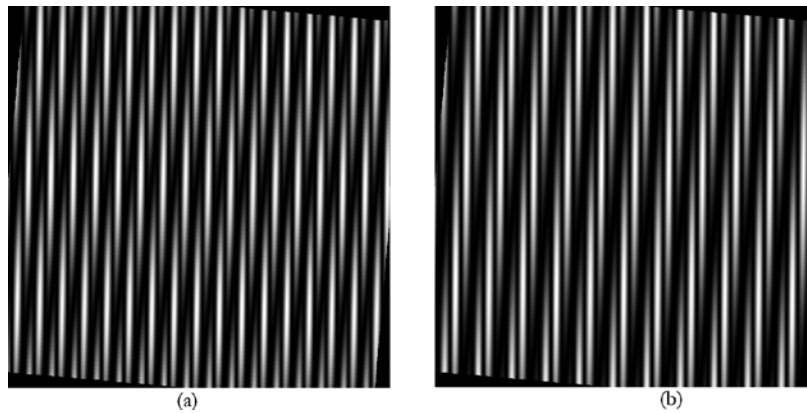


Fig. 4. (a)The multiplicative superposition of two little inclined cosinusoidal gratings with frequency ratio 1:2(b) The multiplicative superposition of two little inclined cosinusoidal gratings with frequency ratio 1:3

Considering the pseudo-moiré of $m = 2$, we substitute m into Eq. (17) and obtain

$$\tan \gamma_p = \tan\left(\frac{\pi - \alpha}{2}\right), \quad P_p = \frac{P_1}{2|\sin(\alpha/2)|}. \quad (19)$$

The angle of the low-frequency fringe of the obtained pseudo-moiré coincides with that in Fig. 3. But the pseudo-moiré in Fig. 4(a) is a little more difficult to discern than the real moiré shown in Fig. 3. In this circumstance, there also exists a high frequency conjugate pseudo-moiré (corresponding to α'). Because of its high frequency and poor illusional contrast, it's difficult to discern by human eyes. Therefore, the high-frequency pseudo-moiré will not be discussed in this paper.

In the like manner, the pseudo-moiré of $m = 3$ appears in the case of the superposition of two little inclined cosinusoidal gratings that one has three times the pitch of the other. The angle of the low-frequency fringe of the obtained pseudo-moiré in Fig. 4(b) coincides with that in Fig. 3. Obviously, the pseudo-moiré of $m = 3$ is hard to be discerned by human eyes. Thus in the following discussion, we will mainly focus on the pseudo-moiré when $m = 2$.

3.3 Little inclined cosinusoidal gratings where one has non-integral times the pitch of the other

For the situation of non-integral frequency, some simple examples are given and compared. According to the simulation mentioned in section 3.2, it is easy to figure out that the low-frequency moiré fringe is hard to be discerned neither in real moiré nor pseudo-moiré when $P_2/P_1 > 3$, so the real moiré and pseudo-moiré are analyzed in three circumstances: $P_2 = 1.1P_1$, $P_2 = 1.5P_1$, $P_2 = 1.9P_1$. Here $\alpha = 5^\circ$, $\alpha' = 175^\circ$, $P_1 = 30$. The fringes are shown below.

(a) $P_2 = 1.1P_1$ and $P_2 = 1.9P_1$

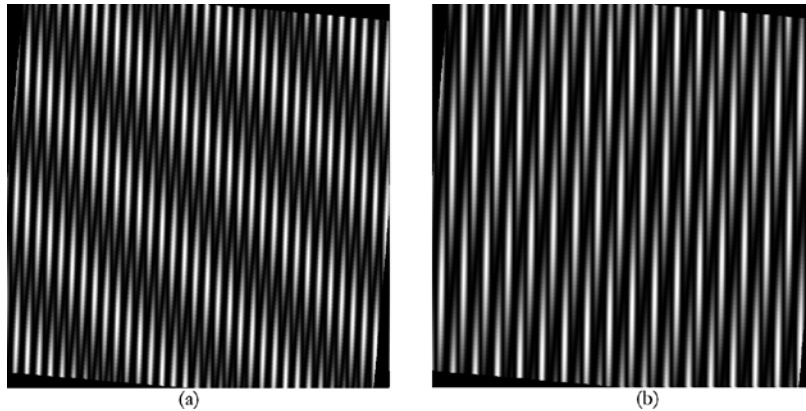


Fig. 5. (a) The multiplicative superposition of two little inclined cosinusoidal gratings with frequency ratio 1:1.1 (b) The multiplicative superposition of two little inclined cosinusoidal gratings with frequency ratio 1:1.9

Angles and periods of real and pseudo-moiré in the case of frequency ratio 1.1 and 1.9 are shown in Table 1. As seen from Fig. 5(a), the low-frequency fringe of real moiré is most prominent. While seen from Fig. 5(b), the low-frequency fringe of pseudo-moiré becomes most prominent.

Table 1. Angles and periods of real and pseudo-moiré in the case of frequency ratio 1.1 and 1.9

Frequency ratio	Real moiré				Pseudo-moiré			
	P_r	$\gamma_r (^\circ)$	P_p	$\gamma_p (^\circ)$	P_r	γ_r	$P_p (^\circ)$	$\gamma_p (^\circ)$
1.1	243.5	40	15.7	2.3	36.3	169	10.7	3.2
1.9	62.8	5.5	19.7	1.7	289.1	117.9	14.6	2.6

(b) $P_2 = 1.5P_1$

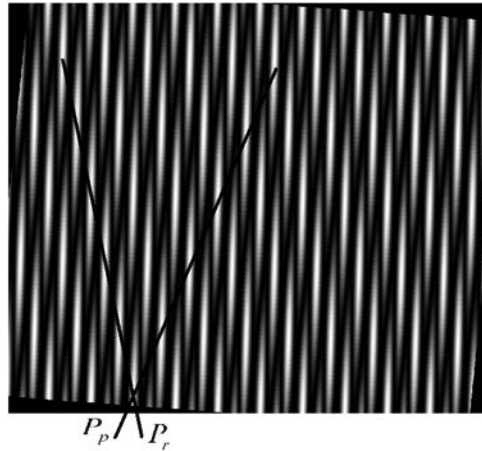


Fig. 6. The multiplicative superposition of two little inclined cosinusoidal gratings with frequency ratio 1:1.5

Angles and periods of real and pseudo-moiré in the case of frequency ratio 1.5 are shown in Table 2. As shown in Fig. 6, the low-frequency fringes of the real moiré and pseudo-moiré have equal strength and both cannot be discerned readily.

Table 2. Angles and periods of real and pseudo-moiré in the case of frequency ratio 1.5

Frequency ratio	Real moiré				Pseudo-moiré			
	P_r	$\gamma_r(^{\circ})$	P_p	$\gamma_p(^{\circ})$	P_r	$\gamma_r(^{\circ})$	P_p	$\gamma_p(^{\circ})$
1.5	88	9.8	18	2	86.2	160.5	12.9	2.9

From the above comparison, we can conclude the coexistence of real moiré and pseudo-moiré. Moreover, the sensitivity of human eyes to real moiré and pseudo-moiré is different in different circumstances. It is easy to conclude that when P_2/P_1 approaches 1, the real moiré is more prominent; when P_2/P_1 approaches 2, the pseudo-moiré becomes more prominent; when $P_2/P_1 = 1.5$, real moiré and pseudo-moiré seem equally to human eyes.

The above discussions on pseudo-moiré produced by two cosinusoidal gratings were carried out in the circumstances of $P_1 < P_2$ and $P_1 \leq P_2$. A universal interpretation can be given below: for any arbitrary P_1 and P_2 , in the case of $P_1/P_2 = r/s$ (r and s are integers and irreducible to each other), when $r = s = 1$, it is real moiré; when $r \neq s$, it is pseudo-moiré. The corresponding items in the Fourier theory are $\pm(r\bar{f}_1 - s\bar{f}_2)$.

4. Discussion on the superposition of two binary gratings

The superposition of two binary gratings relates to four parameters: two periods and two opening ratios. The multiplication of two unidimensional binary waves is complicated, so in the case of the superposition of two binary gratings we list several examples firstly. Finally, the corresponding inferences are given by combining the foregone conclusions with the Fourier theory [6,7,9].

4.1 The superposition of two binary gratings with frequency ratio 1:1 ($P_1 = P_2 = P$)

To analyze the binary gratings' moiré effects based on section 2.2, we first assume the average intensity of the superposition of two periodic square waves having an opening ratio 0.5 and amplitude 1. Therefore, it is easy to figure out that the average intensity of the

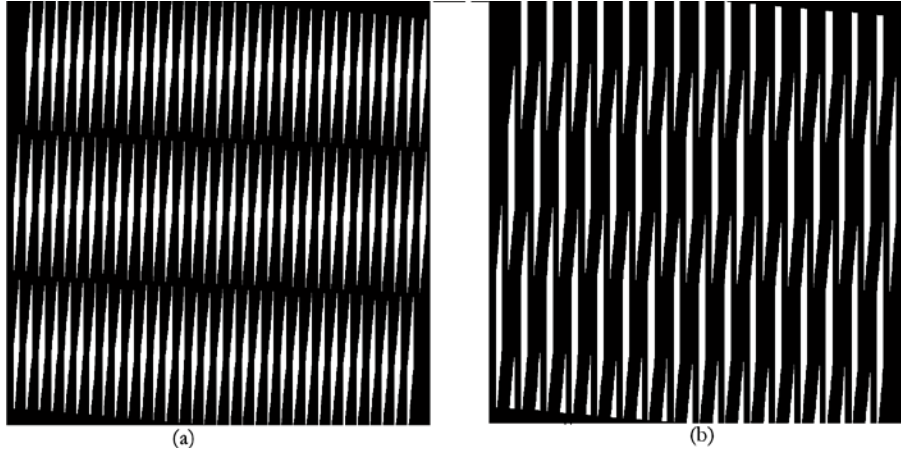


Fig. 7. (a) the multiplicative superposition of two little inclined binary gratings with frequency ratio 1:1 (b) The multiplicative superposition of two binary gratings where the frequency ratio is 1:2 and with little included angle.

superposition with the variation of phase shift φ is $|0.5 - \varphi / p|$. When $\varphi = 0$, the average intensity reaches its maximum value; when $\varphi = P/2$, the average intensity is observed at its minimum. Thus the waveform of the average intensity with variable φ is a triangular wave. So the intensity profile of low-frequency moiré fringe in the Fig. 7(a) is a triangular wave.

Based on partial sum extraction in the Fourier expansions [5,11], the items $\sum_{-n}^n a_n b_n n(\vec{f}_1 - \vec{f}_2)$ in the frequency domain corresponds to a triangular wave. The orientation of the moiré fringe is at one-half the relative inclination of the two gratings. Therefore we can conclude that the waveform of $\sum_{-n}^n a_n b_n n(\vec{f}_1 - \vec{f}_2)$ is the same as the waveform, which is calculated by the interpretation in the image domain. In this case, the interpretation of moiré phenomenon in the image domain coincides with the Fourier theory.

4.2 The superposition of two binary gratings with frequency ratio 1:2 ($2P_1 = P_2$)

According to the Fourier theory, the low-frequency moiré fringe in the Fig. 7(b) reflects the distribution of the superposition of $\sum_{-n}^n a_n b_{2n} n(\vec{f}_1 - 2\vec{f}_2)$. However, b_{2n} equals to zero when the opening ratio is 0.5 [9]. Thus the moiré fringe corresponds to the pseudo-moiré. Utilizing the analysis in section 2.2, we infer that in the orientation of the low-frequency fringe in Fig. 7(b), the equivalent period of the one binary grating is twice the other's. Moreover the average intensity of the superposition of the unidimensional waves is a constant with the variable φ . So the low-frequency fringe that we see is the pseudo-moiré.

The superposition of two binary gratings with an opening ratio 0.5 is similar to the superposition of cosinusoidal gratings. The moiré fringe generated by cosinusoidal gratings is expressed as $r\vec{f}_1 - s\vec{f}_2$. When $r = s = 1$, it corresponds to real moiré; when $r \neq s$, it corresponds to pseudo-moiré. Similarly, the moiré fringe generated by binary gratings is expressed as $\sum_{-n}^n a_n b_{sn} n(r\vec{f}_1 - s\vec{f}_2)$. For the opening ratio 0.5, the real moiré occurs when r and s are both odd numbers, while the pseudo-moiré is produced when r or s is an even number.

4.3 The superposition of two binary gratings with arbitrary periods and opening ratios

Based on discussion mentioned above, the inferences are obtained:

The periods and openings of the two gratings are denoted respectively to T_1 , T_2 , τ_1 , τ_2 , where $\tau_1/T_1 = l_1/k_1$, $\tau_2/T_2 = l_2/k_2$ (l_1 and k_1 are integers and irreducible to each other, and so

are l_2 and k_2). In an arbitrary orientation with an included angle γ , the equivalent periods of the two binary gratings are $T_1' = T_1 / \sin \gamma$ and $T_2' = T_2 / \sin \beta$ with $T_1' / T_2' = i' / k'$ (i' and k' are integers and irreducible to each other). According to the Fourier theory, the corresponding superposition of the family of vectors is $\sum_{-n}^n a_{i'n} b_{k'n} n(\vec{f}_1 - k' \vec{f}_2)$. When $i' = k_1$ or $k' = k_2$ (namely, $a_{i'n} = 0$ or $b_{k'n} = 0$), the superposed fringe is pseudo-moiré. When $k' \neq k_2$ and $i' \neq k_1$ (namely, $a_{i'n} \neq 0$ or $b_{k'n} \neq 0$), it is real moiré.

Utilizing the interpretation it is impossible to analyze every single frequency components of binary gratings. Therefore, calculation is only performed on the waveform of $\sum_{-n}^n a_{i'n} b_{k'n} n(\vec{f}_1 - k' \vec{f}_2)$ in the image domain, but the interpretation can still explain the pseudo-moiré effects of binary gratings visually.

5. Conclusions

In the case of two periodic gratings where frequency ratio and opening ratio are arbitrary, the indicial equation method and Fourier analysis methods are consistent [1]. Indicial equation method involves only the image domain, and only takes into account only the geometric layout of the centerlines of the curvilinear gratings and of the resulting moiré, but it totally ignores their intensity profiles [3,12]. The biggest advantage of the indicial equation method is in its remarkable simplicity, which is particularly welcome in cases where the derivations in the spectral approach become complicated.

The Fourier analysis methods involve the frequency domain and can provide all moiré information including the period, the angle and intensity profile [6,7]. Fourier analysis methods also provide an easy moiré explanation in the case of three or more gratings, including the more complex cases where indicial equation method becomes too complicated. However, in the case of nonlinear gratings, the spectrum of the gratings no longer consists of impulses and may be continuous. It is then impossible to analyze the superposition spectrum with the same ease as before.

Based on the analysis of fluctuations of average intensity of the line families in the image domain, the interpretation of moiré phenomenon in the image domain was proposed. This interpretation explains the pseudo-moiré phenomenon directly in the image domain, with considering both illusional distribution of the average intensity and the human visual system. In the case of two periodic gratings the interpretation of moiré phenomenon has the same meaning as indicial equation method in the image domain. In addition, the interpretation can also provide the information of the phase and the intensity profile of the moiré which cannot be obtained from indicial equation method. Furthermore, our proposed interpretation is consistent with the Fourier theory when two superposed gratings are periodic and provides a visible and understandable analysis method in the image domain.